*Nano Research* 2016, 9(11): 3257–3266
DOI 10.1007/s12274-016-1204-9
**Research Article**
ISSN 1998-0124
CN 11-5974/O4

# Upconversion nano-photosensitizer targeting into mitochondria for cancer apoptosis induction and cyt c fluorescence monitoring

Yanyan Liu[1], Jiawen Zhang[2], Changjing Zuo[3] (✉), Zhen Zhang[4], Dalong Ni[1], Chen Zhang[1], Jing Wang[2], Hui Zhang[4], Zhenwei Yao[2], and Wenbo Bu[1,5] (✉)

[1] *State Key Laboratory of High Performance Ceramics and Superfine Microstructures, Shanghai Institute of Ceramics, Chinese Academy of Sciences, 1295 Dingxi Road, Shanghai 200050, China*
[2] *Department of Radiology, Huashan Hospital, Fudan University, 12 Urumqi Zhong Road, Shanghai 200040, China*
[3] *Department of Nuclear Medicine, Changhai Hospital of Shanghai, 168 Changhai Road, Shanghai 200433, China*
[4] *Cancer Research Institute, Fudan University Shanghai Cancer Center, 270 Dongan Road, Shanghai 200032, China*
[5] *Shanghai Key Laboratory of Green Chemistry and Chemical Processes, School of Chemistry and Molecular Engineering, East China Normal University, 3663 Zhongshan North Road, Shanghai 200062, China*

**Received:** 27 March 2016
**Revised:** 2 July 2016
**Accepted:** 6 July 2016



**KEYWORDS**
mitochondrial reactive oxygen species (mitoROS), upconversion-based photodynamic therapy (PDT), cytochrome c (cyt c), mitochondrial apoptosis

## ABSTRACT

Disruption of mitochondrial reactive oxygen species (mitoROS) plays a major role in cancer cell apoptosis. Here, we designed a core/shell-structured mitochondria-targeting upconversion-based nano-photosensitizer (TPP-UC(PS)) with a lanthanide-doped upconversion nanoparticle (UCNP) core coated by a photosensitizer (PS)-incorporated dense silica shell. Following irradiation with external near-infrared laser (NIR), TPP-UC(PS) in mitochondria caused serious mitochondrial matrix swelling for the activated upconversion-based photodynamic therapy (UC-PDT), and the mobilization of cytochrome c (cyt c) was amplified in response to the increased mitoROS. Specifically, this heme-containing cyt c could be monitored by varying TPP-UC(PS)'s upconversion luminescence signal (UCL), which may facilitate the *in situ* detection of cyt c for apoptosis research. As a proof of concept, our designed TPP-UC(PS) may provide significant opportunities for controlling cancer cell apoptosis under NIR stimulation and for studying apoptosis using the dynamic UCL, which is influenced by local cyt c.

## 1 Introduction

Mitochondria, as one of the most vital subcellular organelles in eukaryotic cells, perform a variety of important functions including energy production, maintenance of calcium homeostasis, activation of

Address correspondence to Changjing Zuo, changjing.zuo@qq.com; Wenbo Bu, wbbu@mail.sic.ac.cn

intracellular signaling, and apoptosis regulation. Insights into these roles have enabled the development of various cancer-fighting strategies such as innovative in anti-cancer drugs, which act to disrupt energy flow or some other vital mitochondrial function or stimulate the formation of reactive oxygen species (ROS), thereby upsetting the redox balance of cellular systems and leading to cancer cell death [1, 2]. Such agents should possess strong selectivity for cancer cells with minimal side-effects on healthy tissues [3, 4]. Strategies for developing suitable mitochondria-targeting antitumor theranostic agents aimed at controlled cancer-cell killing, as well as visual pharmacophore tracing, should be explored.

Since mitochondria are both producers and targets of ROS, mitochondrial reactive oxygen species (mitoROS) production may induce mitochondrial permeability, transition pore opening, decrease the production of adenosine triphosphate (ATP), and, in more severe conditions, upregulate cytochrome c (cyt c), activating mitochondrial death pathways [5]. Since ROS, as the cytotoxic product of photodynamic therapy (PDT), can only migrate less than 0.02 μm after its formation, photodamage can only be generated just at the site or in the close vicinity of photosensitizers (PSs) under irradiation; therefore, the concept of mitochondria-targeting becomes optimal for effective mitochondrial upconversion-based PDT (UC-PDT) [6]. According to the recently developed UC-PDT [7–9], transporting upconversion-based nano-photosensitizers (UC(PSs)) into mitochondria can give a high photochemical mitoROS yield, which is likely to deleteriously affect mitochondrial metabolic pathways and promote cancer cell intrinsic apoptosis. Moreover, the use of NIR laser during UC-PDT can result in great penetration depths, and the NIR-upconverted visible emission enables the direct visual positioning of these upconversion nanoparticle (UCNPs) [10]. Specially, due to the well-matched wavelength between the UCNP upconverted emission (520 nm/545 nm) and absorption of the generated cyt c (520 nm), this UC(PS) becomes a promising candidate for further exploitation as a nano-sensor for monitoring cyt c fluorescence *in situ* [11, 12]. Thus, exploring a mitochondria-targeting upconversion nano-photosensor that manipulates programmed cell death (nano-photosensitizer) and aids in dynamic fluorescence analysis of apoptotic processes (nano-sensor) is of great significance.

To this end, UC(PS) composed of erbium ($Er^{3+}$)-doped UCNP coated with a uniform dense layer of silica loaded with PSs was constructed. Upon NIR excitation at 980 nm, the ensuing fluorescence resonance energy transfer from UCNP to the attached PS resulted in ROS production. When UC(PS) is decorated with the known mitochondria-targeting mitochondriotropic ligand triphenylphosphonium (TPP), the resulting TPP-UC(PS) can freely migrate through the mitochondrial membrane without the requirement for a specific uptake mechanism [13]. Upon NIR excitation, TPP-UC(PS) in mitochondria exhibit enhanced cytotoxicity with upregulated expression of mitochondria-mediated apoptotic genes over the non-targetable group, validating a successful mitochondria-targeting UC-PDT for NIR-induced intrinsic apoptosis. Importantly, the stimulation of mitoROS production contributes to the production and release of cyt c from mitochondria, and the TPP-UC(PS) can also be used as a nano-sensor for sensitive and rapid cyt c monitoring, which could facilitate the real-time detection of cyt c in future apoptosis research.

## 2 Experimental

### 2.1 Material and preparation

All chemicals used in the present experiments were acquired from commercial sources as analytical reagents and used as received without further treatment. UCNPs ($NaYF_4$:18%$Yb^{3+}$/2%$Er^{3+}$) were prepared by our previously reported pyrolysis process [7]. Through a modified oil-in-water reverse microemulsion method, UC(PS) was obtained from the UCNP core by coating with a PS-incorporated dense silica shell [7]. To fabricate TPP-UC(PS), the oppositely charged poly-l-lysine (PLL) was firstly decorated on the surface of UC(PS). The specific process is as follows: 100 μL UC(PS) was added into the PLL solution (1 mL, 1 mg/mL, pH 7.4 PBS buffer containing 0.5 M NaCl) followed by gentle stirring for 20 min. PLL-modified UC(PS) (PLL-UC(PS)) were washed three times followed by resuspension in pure water.

For the final decoration of TPP onto PLL-UC(PS), 17.3 mg EDC and 4.3 mg 3-carboxypropyl triphenylphosphonium bromide (CTPB) were first dissolved into 5 mL methanol, and then 1 mL PLL-UC(PS) in methanol was added. The mixture was stirred overnight, followed by three cycles of centrifugation/redispersion in water to remove residual reactants, and the attachment of TPP groups onto the particle surface (TPP-UC(PS)) was thus accomplished.

### 2.2 Intracellular uptake of NPs detected by confocal laser scanning microscopy (CLSM)

The HeLa human cervical carcinoma cell line was obtained from Beijing Chuanglian North Carolina Biotechnology Research Institute (Beijing, China). Cells were seeded on glass coverslips ($10^4$ cells per slip) and incubated for 12 h. Then, the cells were incubated with the TPP-UC(PS) aqueous dispersion (50 μg/mL, 200 μL) for another 12 h, and washed three times with PBS before mitochondrial staining. MitoTracker Green (Beyotime, China) was dissolved in cell culture medium (72.9 ng/mL) and then 1 mL of the above solution was added onto cells for 30 min before washing off the MitoTracker with PBS. Fluorescence imaging was conducted using CLSM with an Olympus IX81 microscope equipped with a continuous wave NIR laser operating at a wavelength of 980 nm.

### 2.3 ROS detection *in vitro*

HeLa cells (3 × $10^4$ cells/well in 6-well plates) were incubated as described below for the CCK-8 assay. The cells were divided into three groups before treatment with PBS (200 μL), PLL-UC(PS) (50 μg/mL, 200 μL), or TPP-UC(PS) (50 μg/mL, 200 μL) for 12 h. The adherent cells in each treatment group were collected and divided into two groups, one used for 980-nm laser light irradiation (1.5 W/cm$^2$, 10 min), and the other without further treatment. The cells were then washed with serum-free culture medium and resuspended in Dulbecco's Modified Eagle Medium (DMEM) containing 2′,7′-dichlorofluorescin diacetate (DCFH-DA, Beyotime Institute of Biotechnology) (1:1,000) to measure ROS. After 20-min incubation in the dark, cells were twice washed sequentially with DMEM followed by PBS. The fluorescence intensity was assessed by flow cytometry.

### 2.4 Observation of mitochondrial membrane potential ($\Delta\psi_m$)

$\triangle\psi_m$ was determined by JC-1 staining (Beyotime, China) following the manufacturer's instructions. Briefly, the cells were divided into three groups before treatment with PBS (200 μL), PLL-UC(PS) (50 μg/mL, 200 μL), or TPP-UC (PS) (50 μg/mL, 200 μL) for 12 h. The adherent cells in each treatment group were collected and divided into two groups, one used for 980-nm laser light irradiation (1.5 W/cm$^2$, 10 min), and the other without further treatment. The harvested cells were resuspended in a mixture of 500 μL DMEM and 500 μL JC-1 staining fluid, followed by incubation in the dark at 37 °C for 20 min. After washing with ice-cold staining buffer twice by centrifugation, cells were resuspended in 500 μL PBS and analyzed by flow cytometry.

For *in situ* observation, cells were seeded into glass coverslips ($10^4$ cells per slip) and incubated for 12 h. Then, cells were incubated with the aqueous nanoparticle (NP) dispersion (50 μg/mL, 200 μL) for another 12 h, and washed three times with DMEM before JC-1 staining. Lastly, 1 mL PBS was added to each specimen and cells were observed under the laser scan confocal microscope equipped with a 980-nm laser. The $\Delta\psi_m$ staining values after NIR light stimulation were expressed as the ratio of red fluorescence intensity to green fluorescence intensity.

### 2.5 Cyt c detection *in vitro*

HeLa cells were seeded into glass coverslips (at $10^4$ cells per slip) and incubated for 12 h. Then, the cells were incubated with the TPP-UC(PS) aqueous dispersion (50 μg/mL, 200 μL) for another 12 h, and washed three times with PBS. Lastly, 1 mL DMEM was added into the samples and the cells were recultured *in situ*. The intensified intracellular luminescence of UCNP was detected using the 980-nm band pass filter. After introducing cyt c from equine heart, cells were cultured for another 30 min, and the intracellular luminescence of UCNP was further detected. Acetic acid (AA) was added to recover UCNP's green luminescence.

## 3 Results and discussion

### 3.1 TPP-UC(PS) synthesis and characterization

The synthesized UCNPs, UC(PS) and TPP-UC(PS) are shown in Figs. 1(a)–1(c) with high uniformity and mono-dispersity. During the preparation of UC(PS), PS molecules (silicon phthalocyanine dihydroxide, SPCD) can interact with tetraethyl orthosilicate (TEOS) to yield a uniform core/shell structure with the UCNP core coated with a SPCD-incorporated dense silica shell [7, 14, 15]. Furthermore, the broad absorption spectrum of SPCD at 672 nm is derived from its conjugated π bonding system that overlays with the upconversion emissions of UCNPs, allowing efficient energy transfer from the core to the attached PS (Fig. S1 in the Electronic Supplementary Material (ESM)).

For TPP decoration, pre-encapsulation of PLL on UC(PS) is critical. This is because the amino groups in the PLL shell can provide a positive charge and anchoring groups for TPP [16]. As shown in Fig. 1(d), PLL molecules successfully self-assembled on the planar substrates of UC(PS), with a charge reversal from negative to positive. The subsequent conjugation of TPP groups onto PLL-NP surfaces is achieved by a carbodiimide reaction [17]. Those PLL-/TPP-UC(PS) all have outstanding dispersity and stability in water for the well-defined dynamic light scattering (DLS) size distributions over 7 and 30 days, as shown in Fig. 1(e).

### 3.2 TPP-labeled NPs mitochondrial targeting

Cellular uptake of NPs was evaluated with CLSM, as demonstrated by the intensified intracellular luminescence of UCNPs detected using the 980-nm band pass filter (Fig. 2). From the green and red channels, one can see that both the negatively charged UC(PS) and positively charged PLL- or TPP-UC(PS) can be taken up by HeLa cells. To confirm that NPs can successfully target the mitochondria, cells were further treated with MitoTracker Green to indicate mitochondria and the contours of cells. In TPP-UC(PS)-labeled group, the overlap of the fluorescence signals of the MitoTracker and the UCNPs inner core reveals that the TPP-conjugated UC(PS) can specifically target mitochondria, leading to their final accumulation within the mitochondrial matrix. In contrast, the UC(PS)- and PLL-UC(PS)-labeled groups are substantially different, with little overlap of the fluorescent signals of MitoTracker and the NPs. These results demonstrate that TPP decoration endows the UC(PS) with selective mitochondrial targeting function [17].

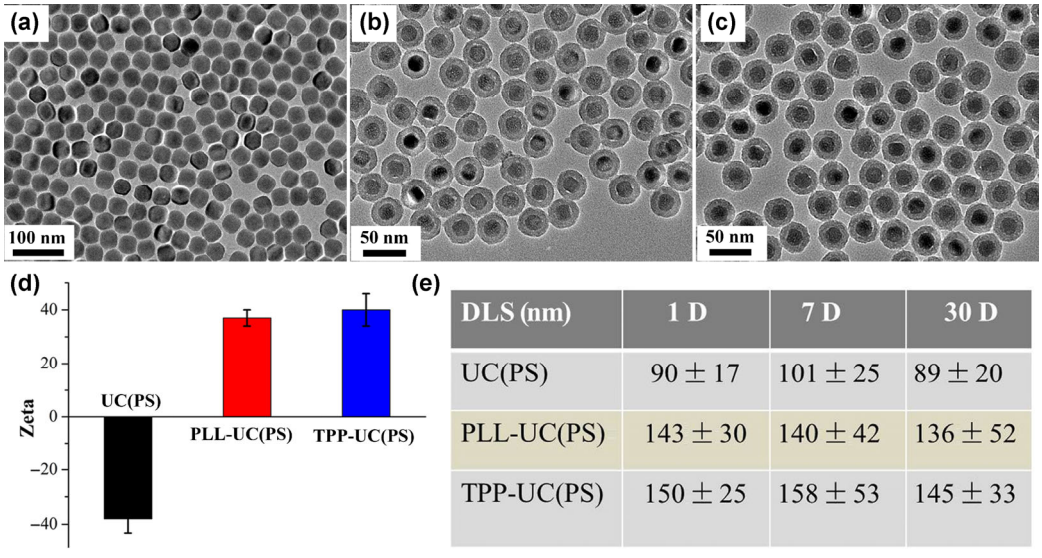


| DLS (nm) | 1 D | 7 D | 30 D |
|---|---|---|---|
| UC(PS) | 90 ± 17 | 101 ± 25 | 89 ± 20 |
| PLL-UC(PS) | 143 ± 30 | 140 ± 42 | 136 ± 52 |
| TPP-UC(PS) | 150 ± 25 | 158 ± 53 | 145 ± 33 |

**Figure 1** (a)–(c) Representative transmission electron microscopic images of UCNP, UC(PS), and TPP-UC(PS). (d) Zeta-potential of UC(PS) nanoparticles with different surface modifications. (e) DLS for UC(PS) nanoparticles with different surface modifications after incubation for 1, 7, or 30 days.

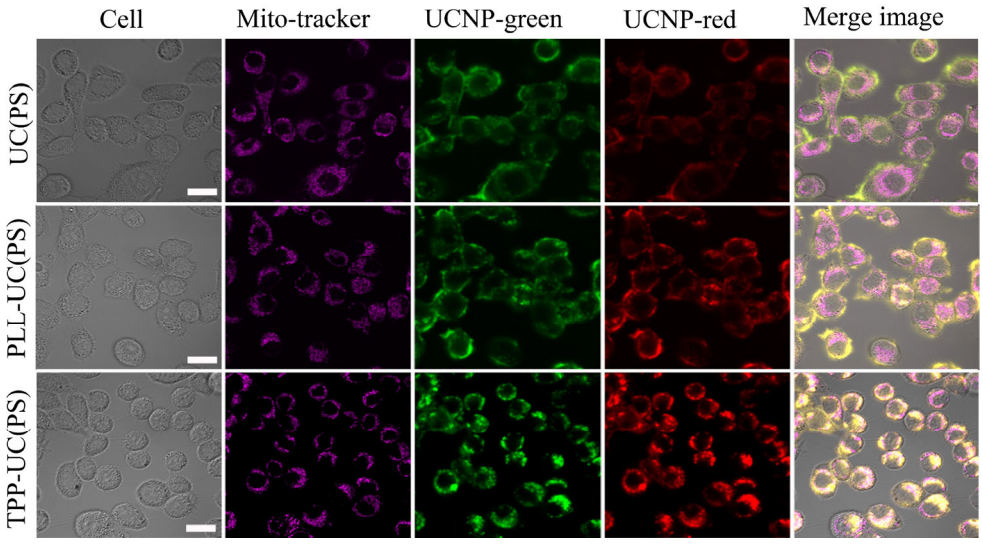


**Figure 2** Confocal fluorescence images of HeLa cells treated with UC(PS), PLL-UC(PS), and TPP-UC(PS). Cells are viewed in the green channel (excitation 980 nm, emission 520–550 nm, green) and the red channel (excitation 980 nm, emission 640–670 nm, red) for UCNP, and the green channel (excitation 488 nm, emission 500–550 nm, the pink color) for MitoTracker Green, respectively. The scale bar represents 20 μm.

### 3.3 Cancer apoptosis induced by intramitochondrial UC-PDT

Cytotoxicity of the TPP-UC(PS) was evaluated by CCK-8 assay. Incubation with 500 μg/mL TPP-UC(PS) for 24 h led to a slight decrease in cell viability (<5%), meaning that the TPP-UC(PS) accumulation in mitochondria has aroused negligible cytotoxicity without light irradiation (Fig. S2 in the ESM). To evaluate therapeutic efficacy of the intramitochondrial UC-PDT, ROS production in cancer cells was first assessed by using DCFH-DA. As shown in Fig. 3(a), no obvious changes in mean fluorescence intensity (MFI) were detected for control experiments treated with or without NIR irradiation, indicating a negligible effect of NIR laser alone on cellular ROS status. Intracellular fluorescence signals were markedly increased after exposure to 980-nm laser in the cells cultured with the NPs, especially for these TPP-UC(PS)-labeled cells, when compared with the cells in the presence of UC(PS) or PLL-UC(PS) under the same conditions. These differences can be attributed to the TPP-UC(PS)'s efficient cellular uptake, easy endosomal escape, and targeted mitochondrial entrapment.

After establishing an effective laser power for ROS production from TPP-UC(PS) in mitochondria, the efficacy of UC-PDT for inducing cell death was further tested. Increased NIR energy exposure time can led to a correspondingly increased cell death rate (death rate around 16.4%, 980-nm laser 1.5 W/cm$^2$ for 10 min). In response to this laser power, TPP-UC(PS) located in mitochondria revealed enhanced cell lethality of 51.8% and 19.31% compared to control and PLL-UC(PS) groups, respectively (Fig. 3(b)). To determine the mode of action, we investigated the anticancer effects of UC-PDT working in varied intracellular organs on the expression of mitochondria-mediated apoptotic genes (pro-apoptotic molecules BAX, cyt c, caspase-3, and cell surface death receptor FAS) [18, 19] by western blotting (Fig. 3(c)). Apoptotic genes were upregulated by UC-PDT of PLL-UC(PS), and further enhanced upon use of mitochondria-targeted TPP-UC(PS). The influence of the TPP-UC(PS) on mitochondrial morphology was also examined through the observation of ultrathin sections of cells by biological transmission electron microscopy (Bio-TEM). As shown in Fig. 3(d), there are great numbers of TPP-UC(PS) accumulated in the mitochondrial matrix with the contours of mitochondria being clearly legible. This result provides convincing evidence that TPP-UC(PS) is highly bio-safe under "dark" conditions. After NIR laser irradiation, most mitochondrial matrices underwent serious swelling and became misshapen due to the significant destruction by generated mitoROS

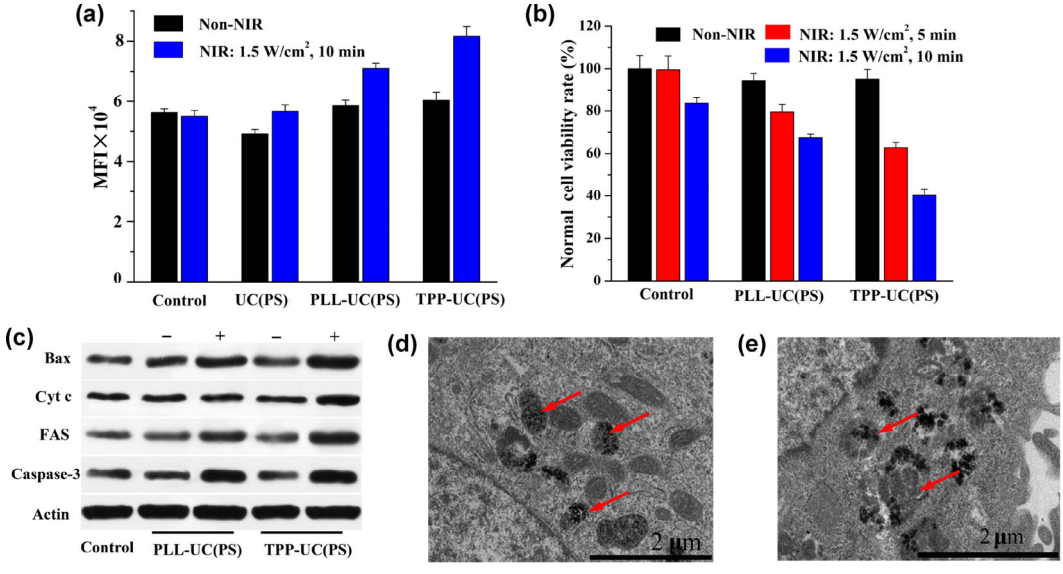


**Figure 3** (a) UC-PDT induced increase of ROS. Flow cytometry was used to measure the MFI of DCF to illustrate the levels of intracellular ROS. (b) Effects of NIR laser stimulus on apoptosis of different nanoparticle-labeled HeLa cells. Cell viability was determined by CCK-8 assay. (c) The expression of death receptors and mitochondria-mediated apoptotic proteins as visualized by western blotting. (d) and (e) Bio-TEM ultrastructures of mitochondria for TPP-UC(PS)-labeled cells before (d) and after (e) NIR light irradiation, showing the typical mitochondrial crista structure and the destroyed mitochondrial structure, respectively.

(Fig. 3(e)). The above results are in accordance with the initial proposal that the UC-PDT conducted in mitochondria will give a higher photochemical yield of mitoROS to deleteriously affect mitochondrial metabolic pathways and promote intrinsic apoptosis of cancer cells.

### 3.4 Evidence for mitochondrial apoptosis

Alterations in $\Delta\psi_m$ can notably affect mitochondrial membrane permeability (MMP), which plays an important role in the release of the pro-apoptotic proteins to trigger caspase activation and cell apoptosis [20]. Therefore, the dissipation of $\Delta\psi_m$ is a general feature of apoptosis, irrespective of the cell type and the apoptosis inducer. Herein, $\Delta\psi_m$ level was monitored in living cells by using the potential-sensitive dye JC-1. As shown in Fig. 4(a)–4(f), compared to the PBS group, cells pre-treated with PLL-UC(PS) or TPP-UC(PS) show a reduced MMP after NIR laser irradiation, as indicated by a decrease in red (JC-1 aggregates)/green (JC-1 monomers) ratio (Fig. S3 in the ESM) [21]. More importantly, the effect of TPP-UC(PS) on $\Delta\psi_m$ was more significant than PLL-UC(PS), which should be attributed to the accurate photodamage of ROS on mitochondria. CLSM imaging also shows that cells subjected to NIR irradiation alone (PBS group) exhibited overwhelming red fluorescence with weak green fluorescence throughout the experiment, suggesting a normal cellular polarization state. While, for cells labeled with PLL-UC(PS) or TPP-UC(PS), the aggregated JC-1 in mitochondria was split into its monomeric forms after NIR laser irradiation, with the red and green fluorescence intensities respectively being increased and decreased, in a time-dependent manner (Fig. 4(g)). These findings are of great significance to understand the roles of ROS produced in mitochondria, which could directly induce MMP and release apoptosis-triggering proteins.

### 3.5 Assay performance on cyt c

Cyt c release from mitochondria represents a major caspase activation pathway, defining the point of irreversible cell apoptosis [22]. Therefore, analyses for these specific molecular players in living cells are critical for apoptosis research. Spectrum analysis shows a pronounced overlap between the emission of UCNPs and the absorption of cyt c (Fig. 5(a)), which can be fortunately used for monitoring cyt c through

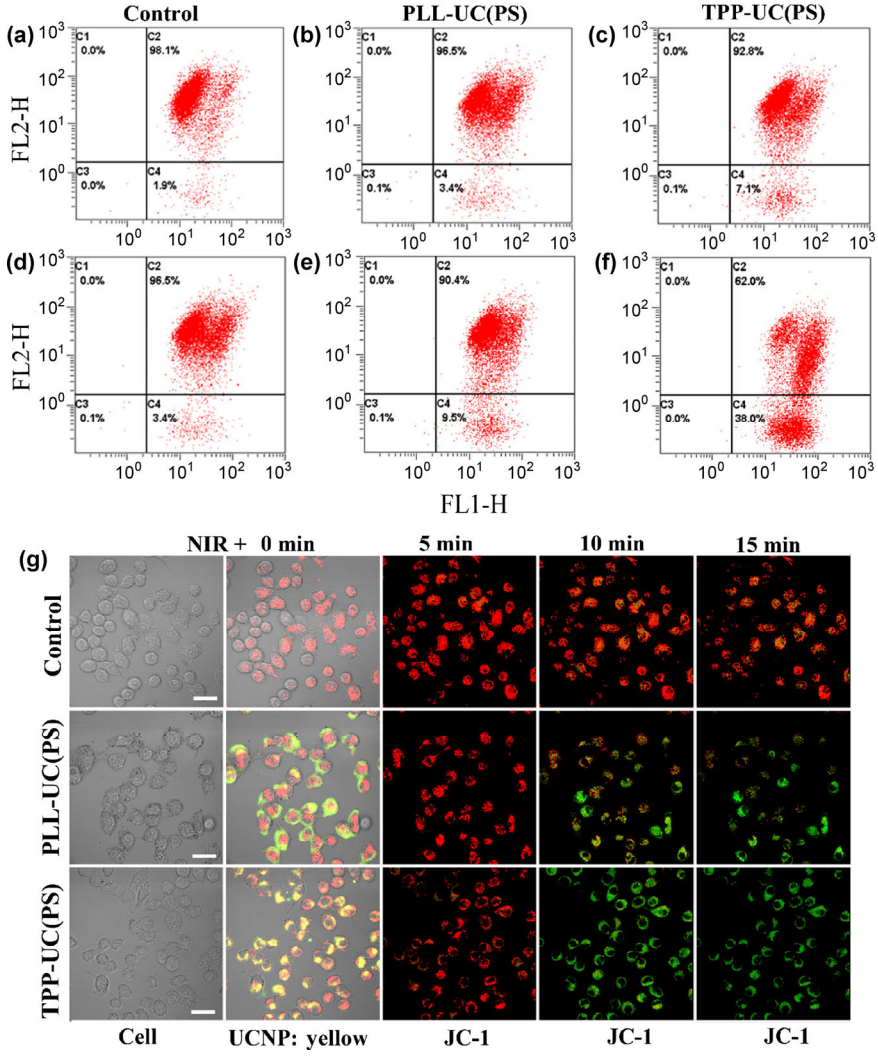


**Figure 4** Efficacy of UC-PDT treatment assessed by quantitative analysis of MMP in HeLa cells labeled with different nanoparticles: (a)–(c) cells without 980-nm NIR light irradiation; (d)–(f) cells exposed to a 1.5 W/cm$^2$ NIR laser for 10 min. FL1-H green, FL2-H red. (g) Confocal fluorescence images of JC-1-stained NPs-labeled HeLa cells under NIR laser stimulus. Each exposure lasted for 5 min. The scale bar is 20 μm.

a potential luminescence resonance energy transfer (LRET) mechanism. To demonstrate this, we added different concentrations of cyt c into the aqueous solution containing as-prepared upconversion nanosensors. As shown in Fig. 5(b), upon the successive addition of cyt c to the solution of TPP-UC(PS), a significant decrease in the UCL intensity at 545 nm ($UCL_{545\ nm}$) can be observed immediately after the addition due to the strong fluorescence absorption efficiency of cyt c, with the UCL at 660 nm ($UCL_{660\ nm}$) remaining relatively stable. To further confirm our hypothesis, AA was introduced to denature cyt c and change its absorbance peaks. It should be noted that the cyt c′ absorption band at 520 nm disappeared after the addition of AA (Fig. 5(c)) [23], and then the originally suppressed UCL by cyt c was recovered due to the final wavelength mismatch between the absorption of degenerated cyt c and the green emission of UCNPs (Fig. 5(d)).

To further investigate the capability of TPP-UC(PS) for monitoring cyt c in cells, HeLa cells were pretreated with TPP-UC(PS) and analyzed under a confocal microscope equipped with a 980 nm laser. Green (545 nm) and red (660 nm) UCLs emitted by TPP-UC(PS) can be clearly observed in cells, indicating the cellular uptake of these nanoparticles. Because of

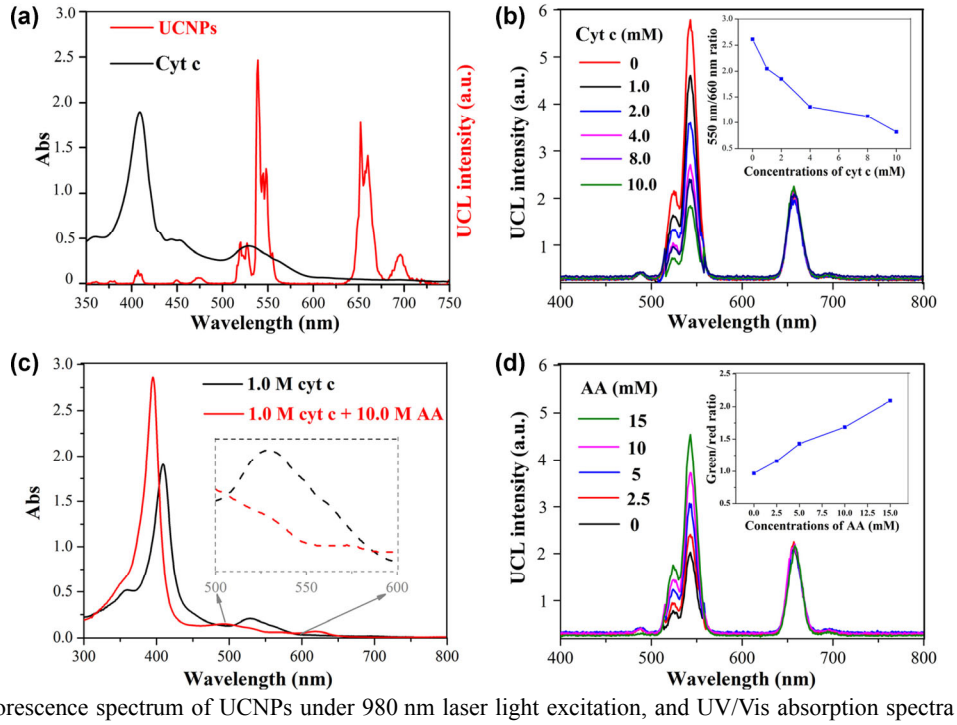


**Figure 5** (a) Fluorescence spectrum of UCNPs under 980 nm laser light excitation, and UV/Vis absorption spectra of cyt c. (b) UCL response of TPP-UC(PS) solutions to cyt c concentration (0–10 mM) in an aqueous solution, inset: plot of luminescence intensity at $UCL_{545\ nm}/UCL_{660\ nm}$ against cyt c concentration. (c) UV/Vis absorption spectra of cyt c upon the addition of AA, inset: partial-enlarged view of the spectrum. (d) Photoluminescence response of TPP-UC(PS)/cyt c solution to the addition of AA, inset: luminescence recovery of $UCL_{545\ nm}$ by adding AA in the range of 0–15 mM.

the insufficient sensitivity of CLSM, the change of upconversion luminescence intensity for μM cyt c in living cells can't be detected (Fig. S4(a) in the ESM). These TPP-UC(PS) pre-treated cells were then co-cultured with cyt c (5 mM) for 30 min, and the green emission turned considerably weak under almost the constant red UCL intensity, suggesting a considerable energy transfer from TPP-UC(PS) to cyt c (Fig. S4(b) in the ESM). Furthermore, this green emission became mostly recovered in another 10 min after the addition of AA (10 mM) as seen in Fig. S4(c) in the ESM. Although the endogenously released cyt c, induced by mitoROS in cells demonstrated by the previous western blotting, leads to invisible UCL change in the confocal images (Fig. S5 in the ESM), this nanoparticle still provides a new opportunity for assaying apoptosis associated with cyt c with ultrasensitive fluorescence detection methodology in the future.

## 4 Conclusion

In summary, a mitochondria-targeting antitumor theranostic agent TPP-UC(PS) has been constructed. Under NIR laser irradiation, TPP-UC(PS) in mitochondria can enhance ROS production, which will destabilize the mitochondria and lead to mitochondrial membrane permeabilization, releasing cyt c and other intermembrane space proteins that trigger apoptotic cell death. In addition, these NPs can further be used as nano-sensors for cyt c detection due to the quenched $UCL_{545\ nm}$ caused by the absorption behavior of cyt c to UCL. Our photo-sensing system may provide a new possibility for controlling phototoxicity and also for studying mitochondrial apoptosis by monitoring cyt c release in cells by employing more sensitive fluorescence detection methodology.

## Acknowledgements

This work has been financially supported by the National Natural Science Foundation of China (Nos. 51372260, 51132009, and 81471714), and the Shanghai Excellent Academic Leaders Program (No. 16XD1404000). Thanks to Linlin Zhang, Heliang Yao, Qingfeng Xiao,

Huaiyong Xing, Wenpei Fan, Zhaowen Cui, Li Jiang, and Jianan Liu from Shanghai Institute of Ceramics, Chinese Academy of Sciences for useful discussions.

**Electronic Supplementary Material**: Supplementary material (adding spectra, cell viability rate, and CLSM) is available in the online version of this article at http://dx.doi.org/10.1007/s12274-016-1204-9.

## References


[1] Gogvadze, V. Targeting mitochondria in fighting cancer. *Curr. Pharm. Des.* **2011**, *17*, 4034–4046.

[2] Fulda, S.; Galluzzi, L.; Kroemer, G. Targeting mitochondria for cancer therapy. *Nat. Rev. Drug Discov.* **2010**, *9*, 447–464.

[3] Jokerst, J. V.; Gambhir, S. S. Molecular imaging with theranostic nanoparticles. *Acc. Chem. Res.* **2011**, *44*, 1050–1060.

[4] Hu, Q. L.; Gao, M.; Feng, G. X.; Liu, B. Mitochondria-targeted cancer therapy using a light-up probe with aggregation-induced-emission characteristics. *Angew. Chem., Int. Ed.* **2014**, *53*, 14225–14229.

[5] Petronilli, V.; Penzo, D.; Scorrano, L.; Bernardi, P.; Di Lisa, F. The mitochondrial permeability transition, release of cytochrome c and cell death. Correlation with the duration of pore openings *in situ*. *J. Biol. Chem.* **2001**, *276*, 12030–12034.

[6] Dougherty, T. J.; Gomer, C. J.; Henderson, B. W.; Jori, G.; Kessel, D.; Korbelik, M.; Moan, J.; Peng, Q. Photodynamic therapy. *J. Natl. Cancer Inst.* **1998**, *90*, 889–905.

[7] Liu, Y. Y.; Liu, Y.; Bu, W. B.; Cheng, C.; Zuo, C. J.; Xiao, Q. F.; Sun, Y.; Ni, D. L.; Zhang, C.; Liu, J. N. et al. Hypoxia induced by upconversion-based photodynamic therapy: Towards highly effective synergistic bioreductive therapy in tumors. *Angew. Chem., Int. Ed.* **2015**, *54*, 8105–8109.

[8] Fan, W. P.; Bu, W. B.; Shen, B.; He, Q. J.; Cui, Z. W.; Liu, Y. Y.; Zheng, X. P.; Zhao, K. L.; Shi, J. L. Intelligent $MnO_2$ nanosheets anchored with upconversion nanoprobes for concurrent pH-/$H_2O_2$-responsive UCL imaging and oxygen-elevated synergetic therapy. *Adv. Mater.* **2015**, *27*, 4155–4161.

[9] Ai, X. Z.; Ho, C. J. H.; Aw, J.; Attia, A. B. E.; Mu, J.; Wang, Y.; Wang, X. Y.; Wang, Y.; Liu, X. G.; Chen, H. B. et al. *In vivo* covalent cross-linking of photon-converted rare-earth nanostructures for tumour localization and theranostics. *Nat. Commun.* **2016**, *7*, 10432.

[10] Idris, N. M.; Gnanasammandhan, M. K.; Zhang, J.; Ho, P. C.; Mahendran, R.; Zhang, Y. *In vivo* photodynamic therapy using upconversion nanoparticles as remote-controlled nanotransducers. *Nat. Med.* **2012**, *18*, 1580–1585.

[11] Toccafondi, C.; Prato, M.; Maidecchi, G.; Penco, A.; Bisio, F.; Cavalleri, O.; Canepa, M. Optical properties of yeast cytochrome c monolayer on gold: An *in situ* spectroscopic ellipsometry investigation. *J. Colloid Interface Sci.* **2011**, *364*, 125–132.

[12] Ishida, M.; Dohmae, N.; Shiro, Y.; Oku, T.; Iizuka, T.; Isogai, Y. Design and synthesis of *de novo* cytochromes c. *Biochemistry* **2004**, *43*, 9823–9833.

[13] Wang, X. H.; Peng, H. S.; Yang, L.; You, F. T.; Teng, F.; Hou, L. L.; Wolfbeis, O. S. Targetable phosphorescent oxygen nanosensors for the assessment of tumor mitochondrial dysfunction by monitoring the respiratory activity. *Angew. Chem., Int. Ed.* **2014**, *53*, 12471–12475.

[14] Liu, Y. Y.; Liu, Y.; Bu, W. B.; Xiao, Q. F.; Sun, Y.; Zhao, K. L.; Fan, W. P.; Liu, J. N.; Shi, J. L. Radiation-/hypoxia-induced solid tumor metastasis and regrowth inhibited by hypoxia-specific upconversion nanoradiosensitizer. *Biomaterials* **2015**, *49*, 1–8.

[15] Qiao, X. F.; Zhou, J. C.; Xiao, J. W.; Wang, Y. F.; Sun, L. D.; Yan, C. H. Triple-functional core–shell structured upconversion luminescent nanoparticles covalently grafted with photosensitizer for luminescent, magnetic resonance imaging and photodynamic therapy *in vitro*. *Nanoscale* **2012**, *4*, 4611–4623.

[16] Shi, X. Y.; Wang, S. H.; Swanson, S. D.; Ge, S.; Cao, Z. Y.; Van Antwerp, M. E.; Landmark, K. J.; Baker, J. R., Jr. Dendrimer-functionalized shell-crosslinked iron oxide nanoparticles for *in-vivo* magnetic resonance imaging of tumors. *Adv. Mater.* **2008**, *20*, 1671–1678.

[17] Wang, X. H.; Peng, H. S.; Yang, L.; You, F. T.; Teng, F.; Tang, A. W.; Zhang, F. J.; Li, X. H. Poly-L-lysine assisted synthesis of core–shell nanoparticles and conjugation with triphenylphosphonium to target mitochondria. *J. Mater. Chem. B* **2013**, *1*, 5143–5152.

[18] Gallego, M. A.; Joseph, B.; Hemstrom, T. H.; Tamiji, S.; Mortier, L.; Kroemer, G.; Formstecher, P.; Zhivotovsky, B.; Marchetti, P. Apoptosis-inducing factor determines the chemoresistance of non-small-cell lung carcinomas. *Oncogene* **2004**, *23*, 6282–6291.

[19] Kumar, R.; Han, J. Y.; Lim, H. J.; Ren, W. X.; Lim, J. Y.; Kim, J. H.; Kim, J. S. Mitochondrial induced and self-monitored intrinsic apoptosis by antitumor theranostic prodrug: *In vivo* imaging and precise cancer treatment. *J. Am. Chem. Soc.* **2014**, *136*, 17836–17843.

[20] Crompton, M. The mitochondrial permeability transition pore and its role in cell death. *Biochem. J.* **1999**, *341*, 233–249.

[21] Ding, F.; Shao, Z. W.; Yang, S. H.; Wu, Q.; Gao, F.; Xiong, L. M. Role of mitochondrial pathway in compression-induced apoptosis of nucleus pulposus cells. *Apoptosis* **2012**, *17*, 579–590.

[22] Chen, T. T.; Tian, X.; Liu, C. L.; Ge, J.; Chu, X.; Li, Y. F. Fluorescence activation imaging of cytochrome c released from mitochondria using aptameric nanosensor. *J. Am. Chem. Soc.* **2015**, *137*, 982–989.

[23] Konermann, L.; Douglas, D. J. Acid-induced unfolding of cytochrome c at different methanol concentrations: Electrospray ionization mass spectrometry specifically monitors changes in the tertiary structure. *Biochemistry* **1997**, *36*, 12296–12302.